

A search for the $Z\gamma$ decay mode of the Higgs boson in pp collisions at $\sqrt{s} = 13$ TeV with the ATLAS detector

Kunlin Ran^{1,2}

On behalf of the analysis team

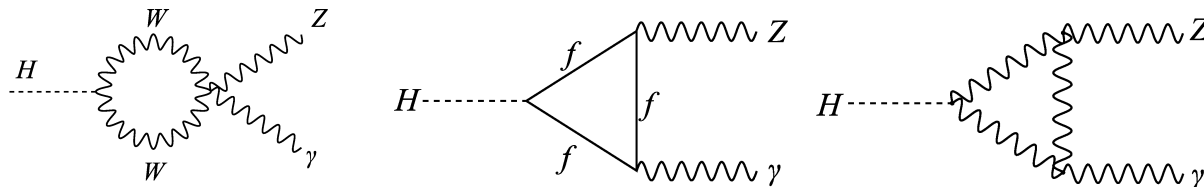
¹IHEP, CAS; ²DESY

CLHCP 2020, 6-9 November

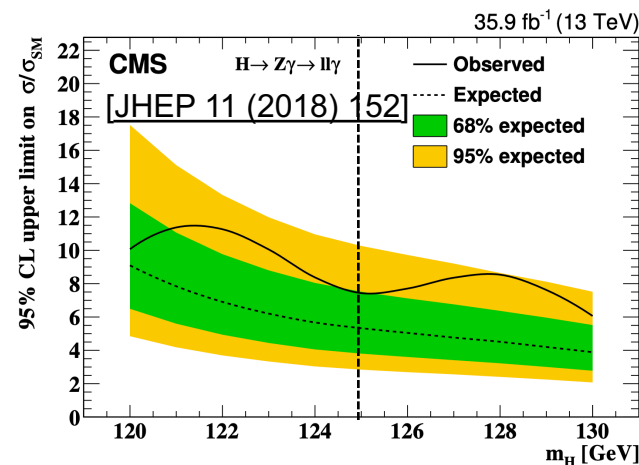
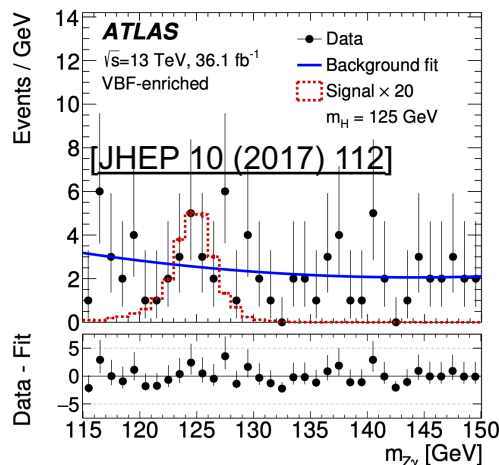


Introduction

- **SM Higgs** can decay into $Z\gamma$ through **loop** diagrams, with predicted $B(H \rightarrow Z\gamma) = (1.54 \pm 0.09) \times 10^{-3}$ at $m_H = 125.09$ GeV; The BR measurements are important for probing the Higgs properties, and for validating SM/BSM theories



- **Z to leptonic decays (e, μ)** can be **efficiently triggered** and **clearly distinguished** from background; In addition, $H \rightarrow Z(\rightarrow ll)\gamma$ can be reconstructed with **good invariant mass resolution** and relatively **small backgrounds**
- In the previous publications, no significant **excess** of events above the **expected background** is observed

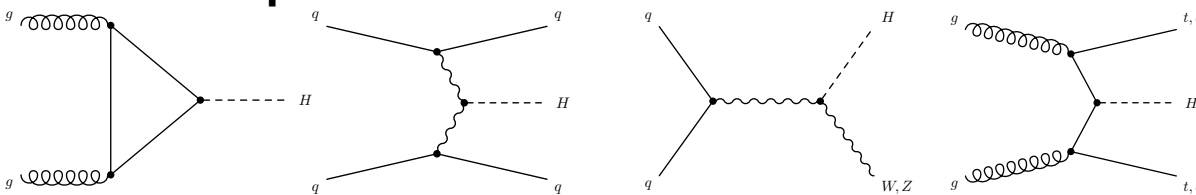


	ATLAS	CMS
Limit of XS x BR at 95% CL	6.6 (5.2) x SM	7.4 (6.0) x SM

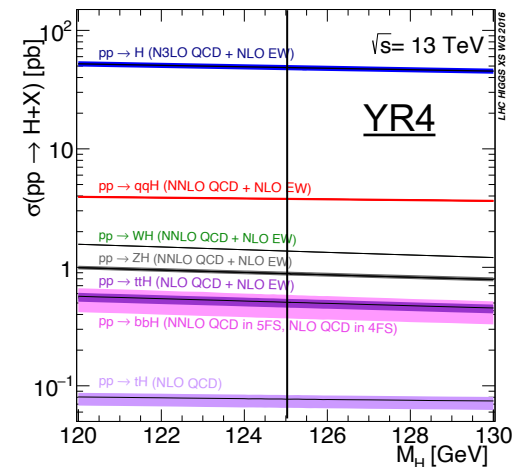
Samples

- An updated search for $H \rightarrow Z(\rightarrow ll)\gamma$ is presented ([Phys. Lett. B 809 \(2020\) 135754](#)) with **full Run2 data (139 fb^{-1})** at the ATLAS experiment, with important improvements
 - Increase in the **size of dataset**
 - Improved **event categorization**
 - Optimized lepton and photon **ID criteria**

MC sample



- **$H \rightarrow Z\gamma$ signal** (PowHeg Pythia8): **ggF, VBF, VH, ttH**
 - **MPIOFF ggF** is used to estimate the **PS** uncertainty
- **$H \rightarrow \mu\mu$** contamination (QED FSR, ~2%): ggF, VBF, VH, ttH
- **Non-resonant Sherpa $Z\gamma$**
- **MG5 EWK $Z\gamma jj$** (orthogonal to Sherpa $Z\gamma$ at parton level)



Object reconstruction, event selection

- Trigger (efficiency: 95.6% for $e\gamma\gamma$; 92.2% for $\mu\mu\gamma$)

Trigger case	Electrons	Muons
Single lepton	$p_{T,\text{lead}} > 27 \text{ GeV}$, $p_{T,\text{sublead}} > 10 \text{ GeV}$	$p_{T,\text{lead}} > 27 \text{ GeV}$, $p_{T,\text{sublead}} > 10 \text{ GeV}$
Dilepton	$p_{T,\text{lead}} > 18 \text{ GeV}$, $p_{T,\text{sublead}} > 18 \text{ GeV}$	$p_{T,\text{lead}} > 24 \text{ GeV}$, $p_{T,\text{sublead}} > 10 \text{ GeV}$

- GRL, Hardest PV, EQ

- Object selection ($\gamma \geq 1$, e or $\mu \geq 2$, OS)

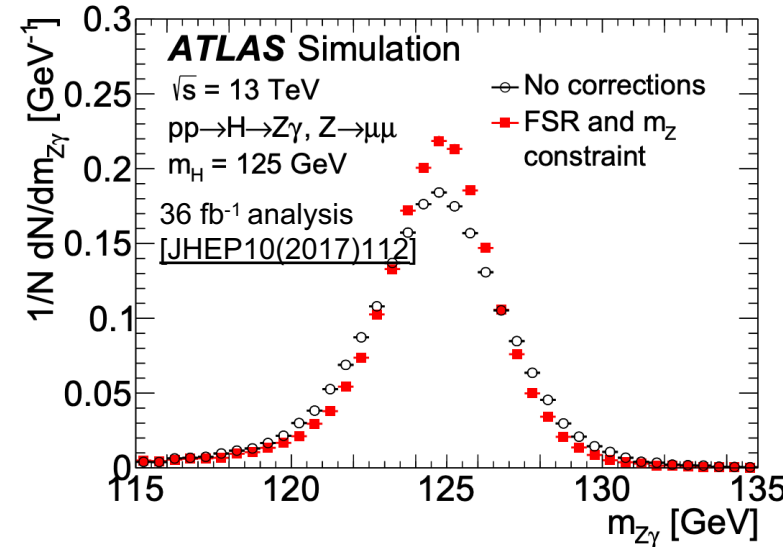
Cut	Electrons	Muons	Photons	
p_T	> 10 GeV	> 10 GeV	> 10 GeV	
$ \eta $	$ \eta < 2.47$	$ \eta < 2.7$	$ \eta < 2.37$	
	exclude $1.37 < \eta < 1.52$	-	exclude $1.37 < \eta < 1.52$	Transition region in EM calorimeter
$ d_0 /\sigma_{d_0}$	< 5	< 3	-	
$z_0 \sin \theta$	< 0.5 mm	< 0.5 mm	-	
Identification	Loose	Medium	Loose	
Isolation	FCLoose	FCLoose	-	

Looser ID cut comparing to the 36 fb^{-1} publication, which was Medium \Rightarrow higher signal acceptance

- Jet
 - EMTopo clusters using anti- k_t algorithm ($\Delta R < 0.4$)
 - $p_T > 25 \text{ GeV}$, $|\eta| < 4.4$
 - JVT cut to suppress pile-up effects (efficiency 92%)
- Overlap removal (selected objects failing angular cuts ($\Delta\eta$, $\Delta\phi$, ΔR) will be discarded)
 - $e - e/\mu$, $\gamma - l$, jet – γ/l

Event selection

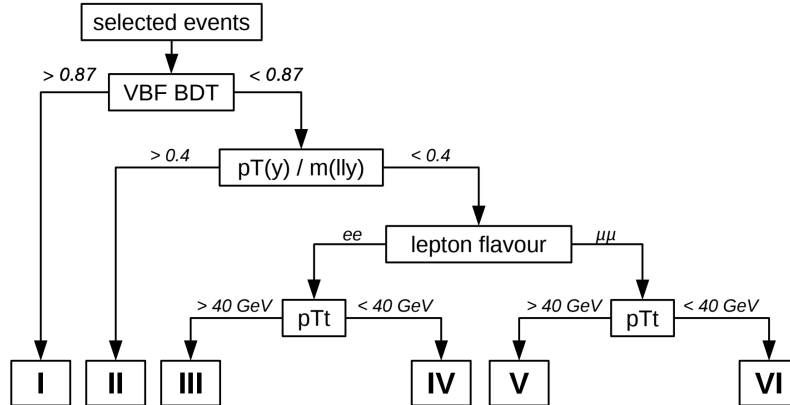
- Z candidate: **OS** ee or $\mu\mu$
 - **$50 < m_{ll} < 101$ GeV before mass resolution correction**
 - **Mass resolution correction (10 ~ 14%)**
 - μ only: FSR correction
 - Kinematic fit correction on m_{ll}
 - **$|m_{ll} - m_Z| < 10$ GeV after mass resolution correction, $m_Z = 91.2$ GeV;**
The **closest** di-lepton pair will be selected



- Trigger match on the selected objects
- Higgs candidate
 - Z candidate + γ with leading p_T
 - **$105 < m_{Z\gamma} < 160$ GeV**
 - $p_T^\gamma/m_{Z\gamma} > 0.12$ to suppress background
- SR: **Tight photon ID, FixedCutLoose isolation**
- Total reconstruction/selection **efficiency on signal:** $20.4\% \pm 2\%$

Categorization

- Events are classified into **6 categories** to improve the **sensitivity** of the signal



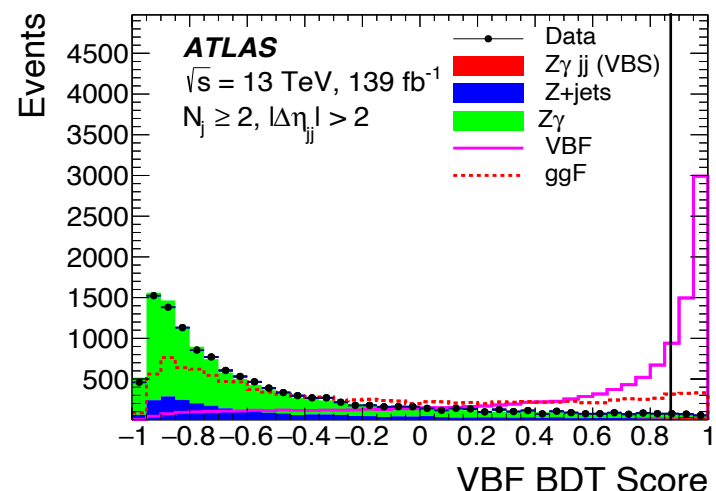
- The **boundaries** of the categories are determined to **maximize the signal significance**

I. VBF-enriched category, trained with **BDT**

- Precut:** $N_j \geq 2$ (2 highest p_T jets are selected), $|\Delta\eta_{jj}| > 2$

Input variable

Variables	Definition
$\Delta\Phi_{Z,\gamma}$	Azimuthal angle between di-lepton system and photon
$\Delta\eta_{jj}$	Pseudo-rapidity separation of dijet
$\Delta R_{\gamma or Z,j}^{\min}$	Minimum ΔR between one object of the Zgamma and jets
m_{jj}	Invariant mass of dijet
p_{Tt}	Zgamma p_T projected perpendicular to the Zgamma thrust axis
$\eta^{Zeppenfeld}$	$ \eta_{Z\gamma} - 0.5 * (\eta_{j1} + \eta_{j2}) $
$\Delta\Phi_{Z\gamma,jj}$	Azimuthal angle between Zgamma and dijet system



Categorization

- Signal efficiency ϵ , fraction f of each production mode per category

Category	ggF		VBF		WH		ZH		$t\bar{t}H$	
	ϵ [%]	f [%]								
VBF-enriched	0.15	27.5	5.1	71.6	0.11	0.5	0.08	0.2	0.07	0.1
High relative p_T	1.1	70.6	2.6	12.9	4.1	7.2	4.1	4.7	7.0	4.6
High p_{Tt} ee	1.7	79.9	2.9	10.8	3.3	4.4	3.4	2.9	3.8	1.9
Low p_{Tt} ee	6.8	93.6	3.5	3.8	3.5	1.3	3.7	0.9	3.1	0.4
High p_{Tt} $\mu\mu$	2.0	79.7	3.6	11.1	4.0	4.4	4.1	2.9	4.3	1.7
Low p_{Tt} $\mu\mu$	8.6	93.6	4.4	3.7	4.5	1.4	4.6	0.9	3.5	0.4
Total efficiency (%)	20.3		22.2		19.5		19.9		21.9	
Expected events	142		12.1		3.8		2.2		1.6	

- Expected signal significance

Category	Events	S_{68}	B_{68}	w_{68} [GeV]	S_{68}/B_{68} [10^{-2}]	$S_{68}/\sqrt{S_{68} + B_{68}}$
VBF-enriched	194	2.7	18.7	3.7	14.3	0.58
High relative p_T	2276	7.6	112.8	3.7	6.7	0.69
High p_{Tt} ee	5567	9.9	444.0	3.8	2.2	0.46
Low p_{Tt} ee	76 679	34.5	6654.1	4.1	0.5	0.42
High p_{Tt} $\mu\mu$	6979	12.0	610.8	3.9	2.0	0.48
Low p_{Tt} $\mu\mu$	100 876	43.5	8861.5	4.0	0.5	0.46
Inclusive	192 571	110.2	16 701.9	4.0	0.7	0.85

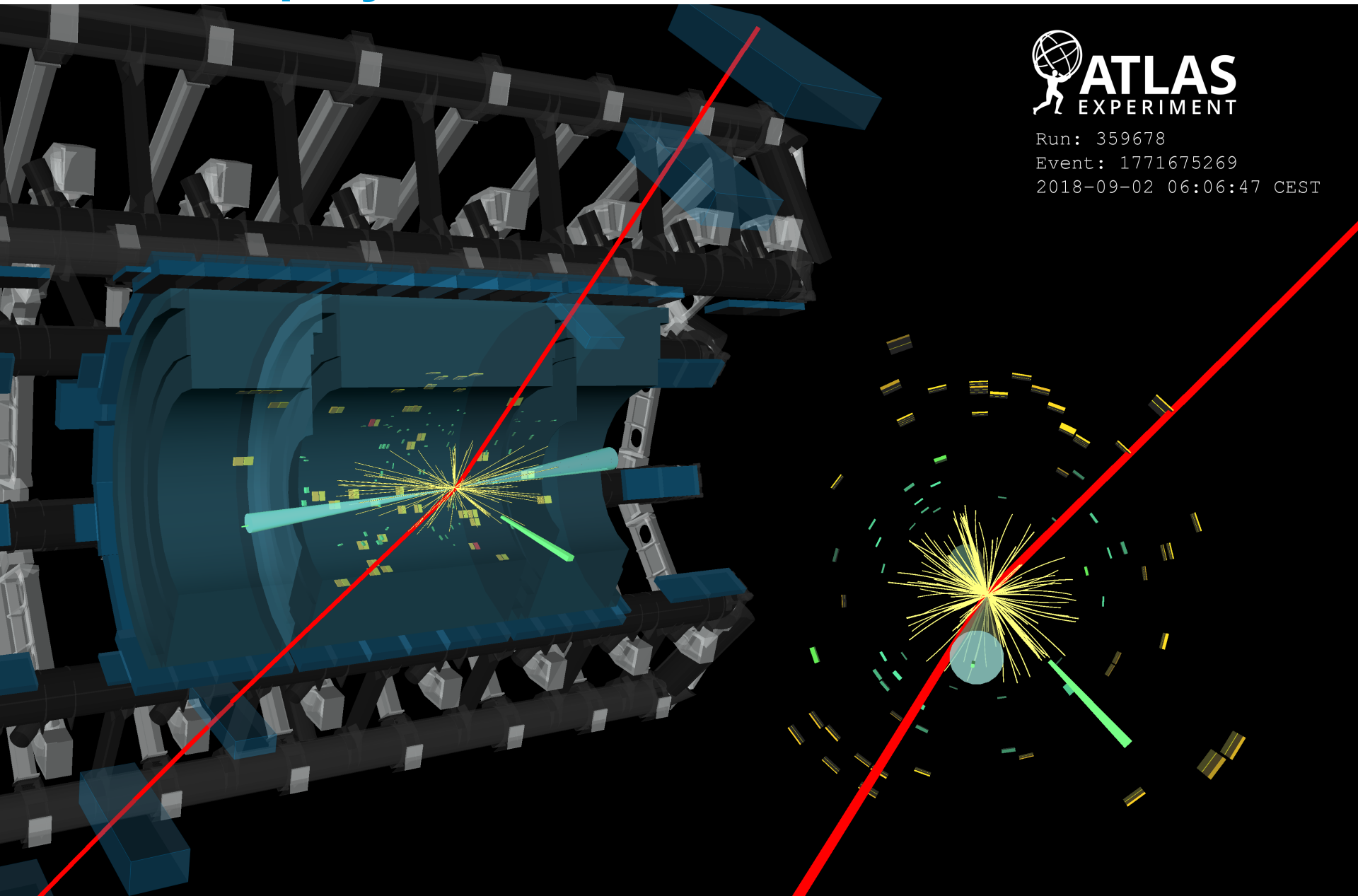
$\sum Z_i^2 = 1.3$

- Continuum $Z\gamma$ background has on average lower p_T of candidate than the signal \Rightarrow higher signal significance in the VBF-enriched, high relative p_T , high p_{Tt} categories
- The categorization improves the sensitivity by $\sim 50\%$ than the inclusive case

Event display of a VBF-enriched candidate

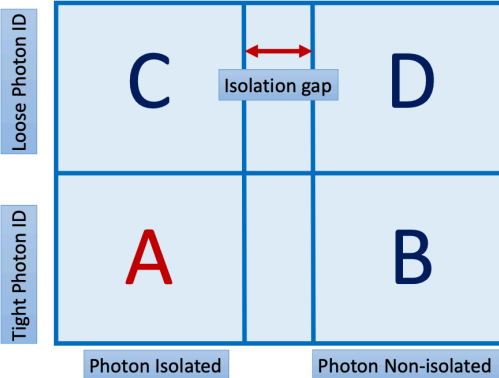


Run: 359678
Event: 1771675269
2018-09-02 06:06:47 CEST



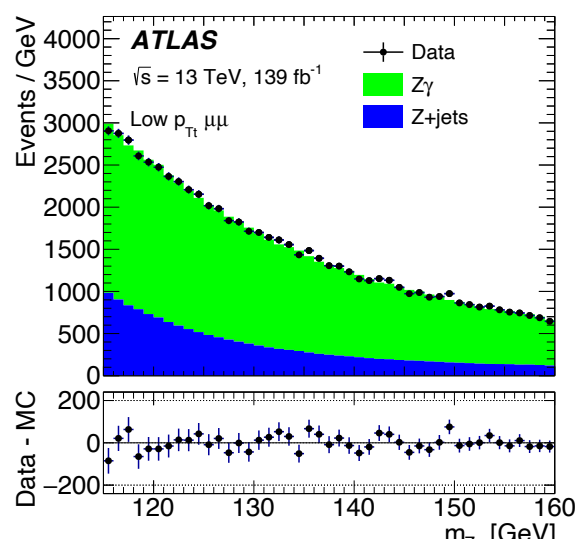
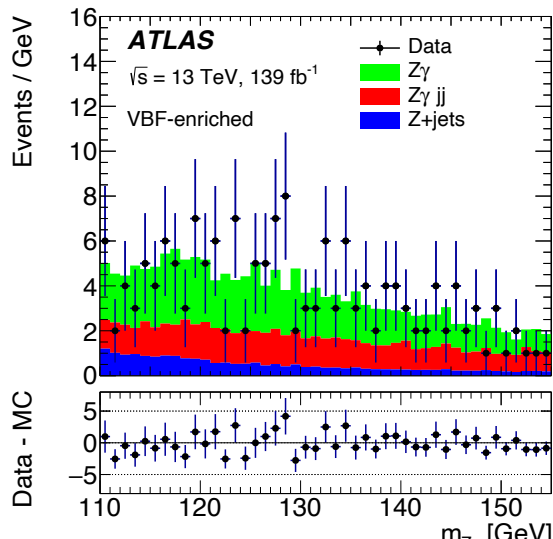
Background composition

- **Background components:** dominant $Z\gamma$, secondary $Z + j$ where jet is misidentified at photon
- **2D sideband method** is applied to estimate **fractions of background components** based on photon ID/ISO performances



- $N_A^{Z\gamma} = N_A^{data} - (N_B^{data} - c_B N_A^{Z\gamma}) \frac{(N_C^{data} - c_C N_A^{Z\gamma})}{(N_D^{data} - c_D N_A^{Z\gamma})} R^{Zj}$
- $c_K \equiv N_K^{Z\gamma} / N_A^{Z\gamma}$, $Z\gamma$ leakage fractions extracted from $Z\gamma$ MC
- $R^{Zj} \equiv \frac{N_A^{Zj} N_D^{Zj}}{N_B^{Zj} N_C^{Zj}}$, jet correlation factor between photon ID/ISO regions;
Obtained from “prime” region data (fail photon ISO)
- The fraction of $Z\gamma$ background in inclusive case is $0.78^{+0.04}_{-0.09}$

- **Data VS background template** with background fraction applied

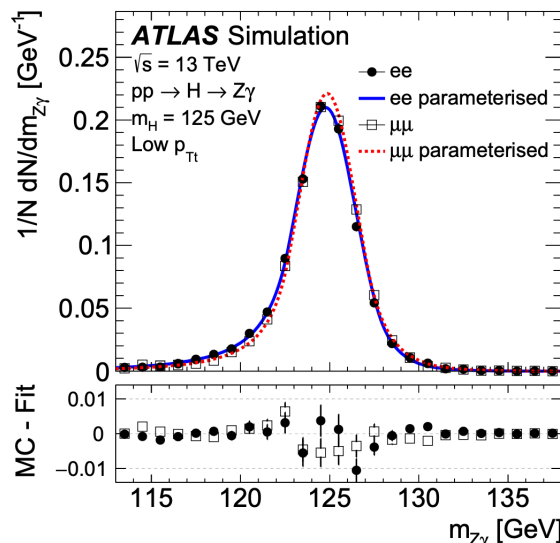


Signal modelling

- The signal and background will be extracted from $m_{Z\gamma}$ fit in data, assuming **parametric models** for signal and background
- Signal**
 - Acceptance and parameters** of the shape are obtained from **MC**
 - Well modeled by **DSCB** function

$$N \cdot \begin{cases} e^{-t^2/2} & \text{if } -\alpha_{Lo} \leq t \leq \alpha_{Hi} \\ \frac{e^{-0.5\alpha_{Lo}^2}}{\left[\frac{\alpha_{Lo}}{n_{Lo}} \left(\frac{n_{Lo}}{\alpha_{Lo}} - \alpha_{Lo} - t \right) \right]^{n_{Lo}}} & \text{if } t < -\alpha_{Lo} \\ \frac{e^{-0.5\alpha_{Hi}^2}}{\left[\frac{\alpha_{Hi}}{n_{Hi}} \left(\frac{n_{Hi}}{\alpha_{Hi}} - \alpha_{Hi} + t \right) \right]^{n_{Hi}}} & \text{if } t > \alpha_{Hi}, \end{cases}$$
$$\Delta m_H = m_{Z\gamma} - \mu_{CB}$$
$$t = \Delta m_H / \sigma_{CB}$$

36 fb⁻¹ analysis
[JHEP10(2017)112]



Background modelling

- **Background models** are chosen using **template**, **value of parameters** are determined by fitting $m_{Z\gamma}$ in **data**
- **Template: MC $Z\gamma + Z\gamma jj$, data-driven $Z + j$** (data CR failing photon tight ID), normalized to data with background fractions respectively
- The choice of **analytical model** and $m_{Z\gamma}$ **fit range** are optimized with **spurious signal (SP) method**
 - Perform **S+B** fit to $m_{Z\gamma}$ **background-only** distribution, scan “signal” in [123, 127] GeV
 - The **maximum** number of “signal” is taken as **SP uncertainty**
 - **Criteria** when selecting background function: $N_{SP} < 50\% \cdot \delta S$ (statistical signal uncertainty); Background only fit $P(\chi^2) > 1\%$
 - The optimal **fit range** and **function** are selected to achieve the **highest signal significance** while fitting the expected **S+B** $m_{Z\gamma}$ distribution, including the **SP uncertainty**

Category	Function Type	Fit range [GeV]
VBF-enriched	Second-order power function	110–155
High relative p_T	Second-order exponential polynomial	105–155
ee high p_{Tt}	Second-order Bernstein polynomial	115–145
ee low p_{Tt}	Second-order exponential polynomial	115–160
$\mu\mu$ high p_{Tt}	Third-order Bernstein polynomial	115–160
$\mu\mu$ low p_{Tt}	Third-order Bernstein polynomial	115–160

Systematic uncertainties

Experimental

Sources	$H \rightarrow Z\gamma$
<i>Luminosity [%]</i>	
Luminosity	1.7
<i>Signal efficiency [%]</i>	
Modelling of pile-up interactions	0.0–0.2
Photon identification efficiency	0.8–1.8
Photon isolation efficiency	0.7–1.9
Electron identification efficiency	0.0–2.3
Electron isolation efficiency	0.0–0.1
Electron reconstruction efficiency	0.0–0.5
Electron trigger efficiency	0.0–0.1
Muon selection efficiency	0.0–0.6
Muon trigger efficiency	0.0–1.6
Jet energy scale	0.0–3.5
Jet resolution	0.0–15
Jet pile-up	0.0–7.5
Jet flavor	0.0–11
<i>Signal modelling on σ_{CB} [%]</i>	
Electron and photon energy resolution	0.5–3.4
Muon – Inner detector resolution	0.0–1.2
Muon – Muon spectrometer resolution	0.0–3.4
<i>Signal modelling on μ_{CB} [%]</i>	
Electron and photon energy scale	0.09–0.15
Muon momentum scale	0.0–0.03
Higgs boson mass measurement	0.19
<i>Background modelling [number of spurious signal events]</i>	
Spurious signal	1.5–39 Dominant: 28%

Theoretical

Sources	
<i>Total cross-section and efficiency [%]</i>	
ggF Underlying event	1.3
perturbative order	4.7–9.6
PDF and α_s	1.8–2.8
$B(H \rightarrow Z\gamma)$	5.7
Total (total cross-section and efficiency)	7.5–11
<i>Category acceptance [%]</i>	
ggF Underlying event	0.1–11
ggF H p_T perturbative order	0.3–0.4
ggF in VBF-enriched category	37
ggF in high relative p_T category	21
ggF in other categories	10–15
Other production modes	1.0–15
PDF and α_s	0.4–3.5
Total (category acceptance)	11–37

- Uncertainty from $H \rightarrow \mu\mu$ contamination: 2.1%
- All **systematics** have secondary contributions on the **total uncertainty** due to **large statistical error (80%)**

Statistical procedures

- A **profile-likelihood-ratio** test statistic is used to search for a signal excess above the background by fitting on $m_{Z\gamma}$

$$\mathcal{L}((\mu, \theta) \mid \{m_{Z\gamma}^i\}_{i=1..n}) = \underbrace{\frac{e^{-N(\mu, \theta)} N^n(\mu, \theta)}{n!}}_{\text{Poisson term}} \underbrace{\left(\prod_{i=1}^n f_{\text{tot}}(m_{Z\gamma}^i, \mu, \theta) \right)}_{\text{PDF of } m_{Z\gamma} \text{ distribution}} \times \boxed{G(\theta) \text{ Constraint term of NP}}$$

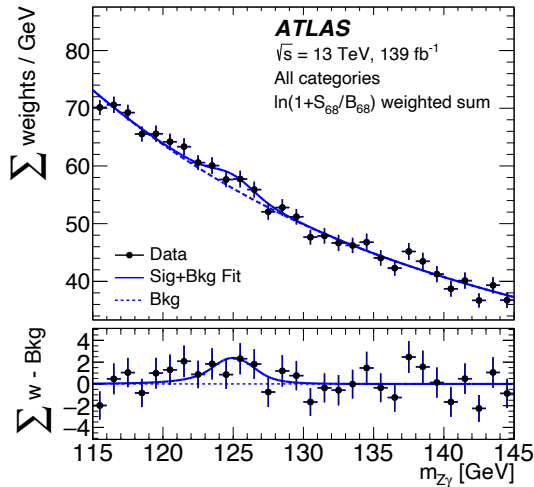
$$f_{\text{tot}}(m_{Z\gamma}^i, \mu, \theta) = \frac{1}{N} \sum_c \left\{ \left[N_{\text{sig}}^{(c)}(m_X, \mu, \theta_{\text{sig}}) + N_{\text{spur}}^{(c)}(m_X, \theta_{\text{spur}}) \right] \times f_{\text{sig}}^{(c)}(m_{Z\gamma}^i, \theta_{\text{sig}}) \right. \\ \left. + N_{H\mu\mu}^{(c)}(m_X, \theta_{H\mu\mu}) \times f_{H\mu\mu}^{(c)}(m_{ll\gamma}^i) + N_{\text{bkg}}^{(c)} \times f_{\text{bkg}}^{(c)}(m_{Z\gamma}^i, \theta_{\text{bkg}}) \right\}$$

- Upper limits** are set on $\sigma(pp \rightarrow H) \times B(H \rightarrow Z\gamma)$ at **95% CL** using asymptotic approximation

$$\tilde{q}_\mu = \begin{cases} -2 \ln \tilde{\lambda}(\mu) & \text{for } \mu \geq \hat{\mu} \\ 0 & \text{for } \mu < \hat{\mu} \end{cases} \quad \text{with} \quad \tilde{\lambda}(\mu) = \begin{cases} \ln \frac{L(\mu, \hat{\theta}(\mu))}{L(\hat{\mu}, \hat{\theta})} & \text{for } \hat{\mu} \geq 0 \\ \ln \frac{L(\mu, \hat{\theta}(\mu))}{L(0, \hat{\theta}(0))} & \text{for } \hat{\mu} < 0 \end{cases}$$

Result

- **Weighted sum plot of all categories with fitted S+B model**



- $\mu = \frac{\sigma \times B}{(\sigma \times B)^{SM}} = 2.0 \pm 0.9(\text{stat.})^{+0.4}_{-0.3}(\text{syst.}) = 2.0^{+1.0}_{-0.9}(\text{tot.})$
- Expected $\mu = 1.0 \pm 0.8(\text{stat.}) \pm 0.3(\text{syst.})$
- **95% CL limit on μ :** 3.6 (2.6) \times SM, assuming **SM Higgs decays to $Z\gamma$** in the expected results
- **95% CL limit on $\sigma(pp \rightarrow H) \times B(H \rightarrow Z\gamma)$:** 305 fb
- **95% CL limit on $B(H \rightarrow Z\gamma)$:** 0.55% , assuming SM Higgs production XS
- Total uncertainty is dominated by **statistical error**
- Dominant **systematics: SP uncertainty**
- Besides the increase in size of the dataset, there're **extra 20% improvement in expected sensitivity** compared with the 36 fb^{-1} publication due to **improved analysis strategy** (optimal object recommendation, improved categorization, ...)

Category	μ	Significance
VBF-enriched	$0.5^{+1.9}_{-1.7} (1.0^{+2.0}_{-1.6})$	0.3 (0.6)
High relative p_T	$1.6^{+1.7}_{-1.6} (1.0^{+1.7}_{-1.6})$	1.0 (0.6)
High $p_{T_t} ee$	$4.7^{+3.0}_{-2.7} (1.0^{+2.7}_{-2.6})$	1.7 (0.4)
Low $p_{T_t} ee$	$3.9^{+2.8}_{-2.7} (1.0^{+2.7}_{-2.6})$	1.5 (0.4)
High $p_{T_t} \mu\mu$	$2.9^{+3.0}_{-2.8} (1.0^{+2.8}_{-2.7})$	1.0 (0.4)
Low $p_{T_t} \mu\mu$	$0.8^{+2.6}_{-2.6} (1.0^{+2.6}_{-2.5})$	0.3 (0.4)
Combined	$2.0^{+1.0}_{-0.9} (1.0^{+0.9}_{-0.9})$	2.2 (1.2)

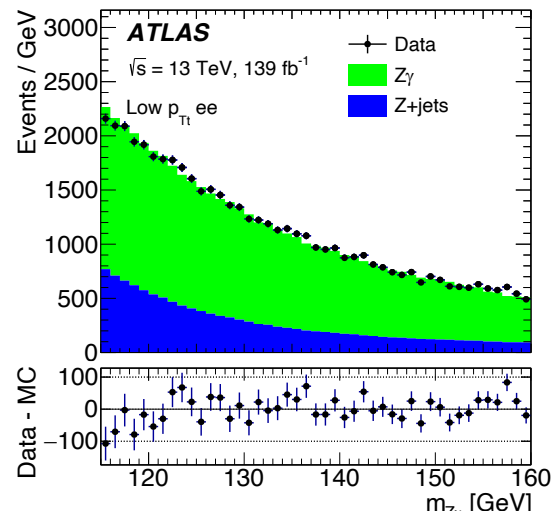
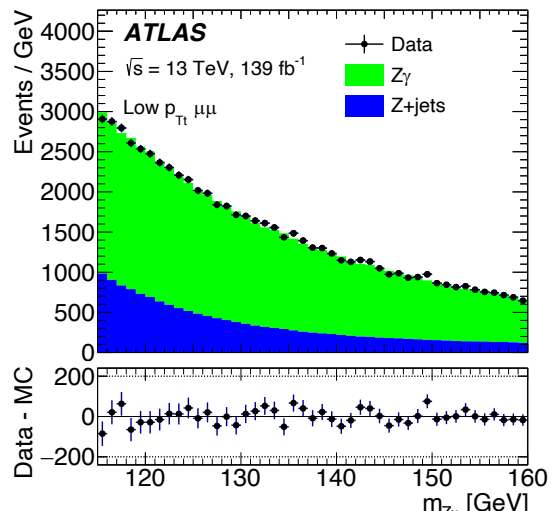
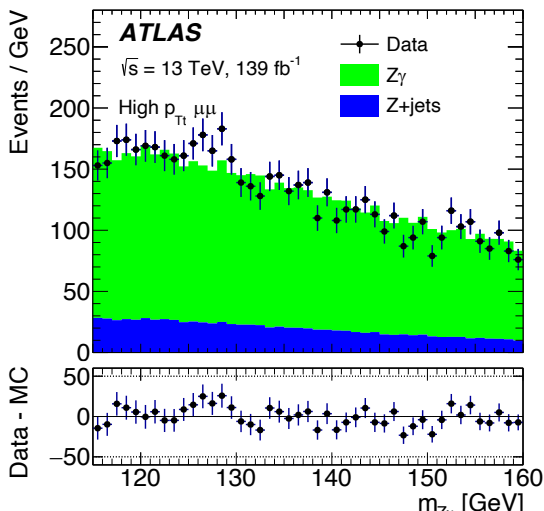
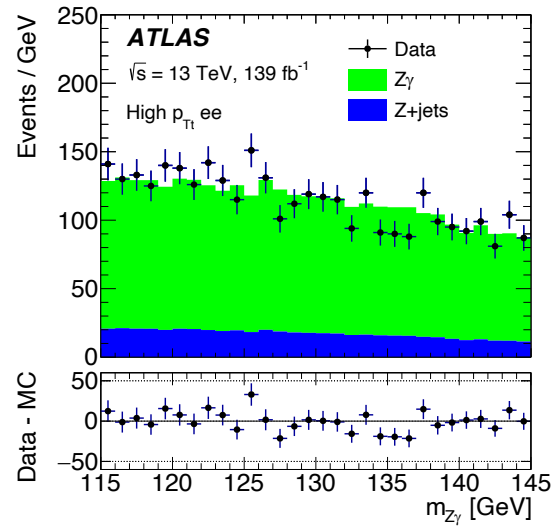
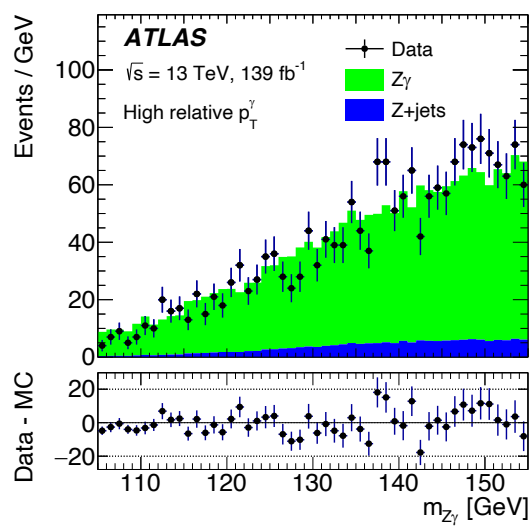
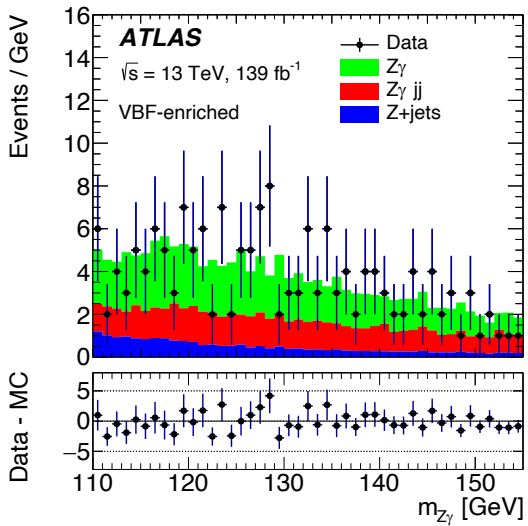
Signal strength compatibility
amongst all categories: p -value 77%

Summary

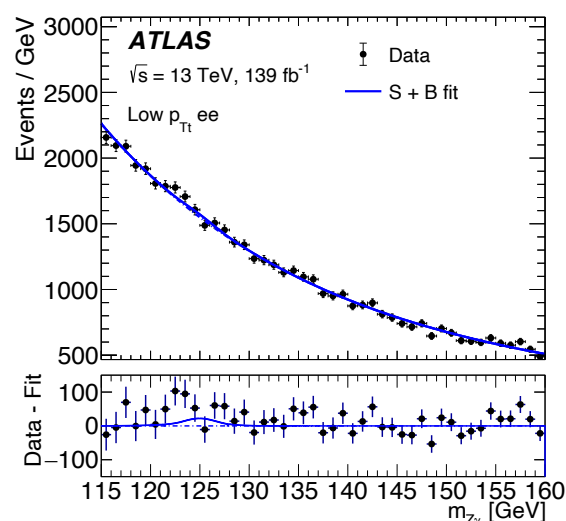
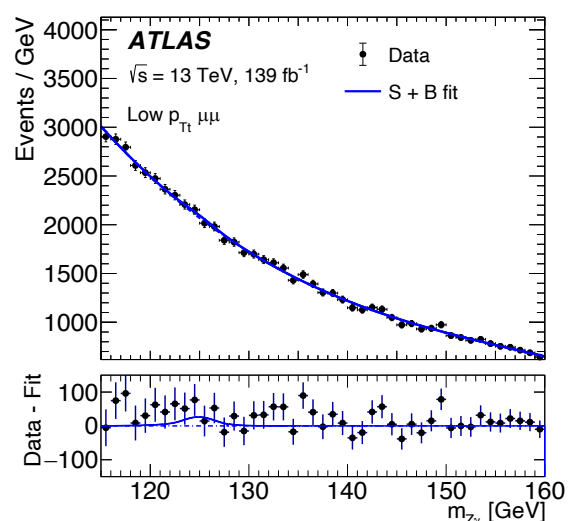
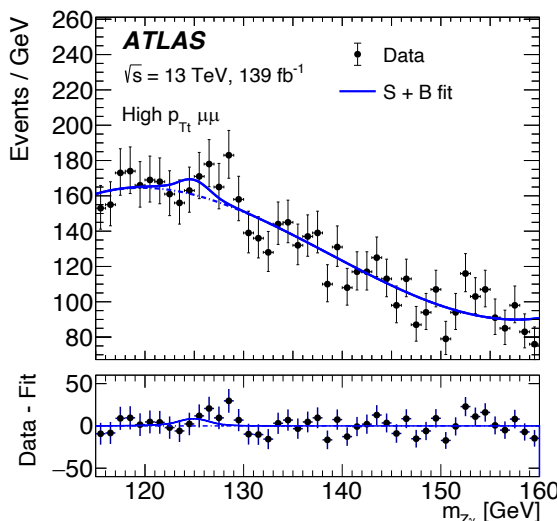
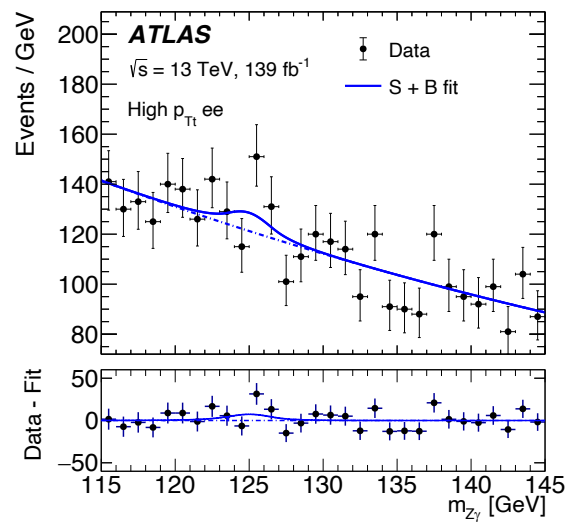
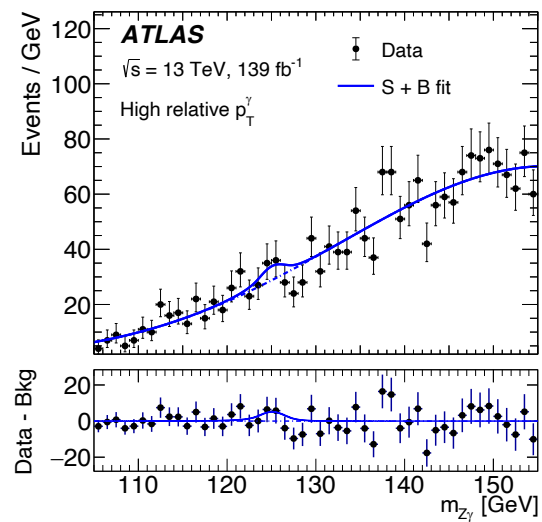
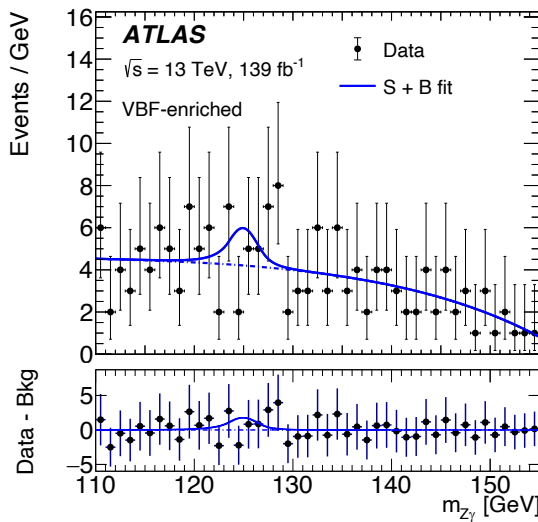
- A search for **SM** $H \rightarrow Z\gamma$ decay with 139 fb^{-1} dataset recorded by the ATLAS detector is presented in [Phys. Lett. B 809 \(2020\) 135754](#)
- $\mu = \frac{\sigma \times B}{(\sigma \times B)^{SM}} = 2.0^{+1.0}_{-0.9} (\text{tot.})$, where the **statistical uncertainty** is dominant
- The **observed** data are consistent with the expected **background** with a *p*-value of 1.3% (**significance**: 2.2σ); The **expected p-value** is 12.3% (**significance**: 1.2σ)
- The **observed 95% CL upper limit** on the $\sigma(pp \rightarrow H) \cdot B(H \rightarrow Z\gamma)$ is $3.6 \times \text{SM}$ for $m_H = 125.09 \text{ GeV}$; The **expected limit** assuming **SM** $H \rightarrow Z\gamma$ decay is $2.6 \times \text{SM}$
- There're **extra 20% improvement** in **expected sensitivity** compared with the 36 fb^{-1} publication just from **the optimized analysis strategy**

Backup

Data VS background template



S+B fit in data



HL-LHC projection

